Biomaterials 86 (2016) 56–67

Contents lists available at ScienceDirect

Biomaterials

journal homepage: www.elsevier.com/locate/biomaterials

Multi-stage inhibition in breast cancer metastasis by orally active triple conjugate, LHTD4 (low molecular weight heparin-taurocholate-tetrameric deoxycholate)

Farzana Alam [a], Taslim A. Al-Hilal [b], Jooho Park [c], Jeong Uk Choi [c], Foyez Mahmud [a], Jee-Heon Jeong [d], In-San Kim [b], Sang Yoon Kim [b, e], Seung Rim Hwang [f, **], Youngro Byun [a, c, *]

[a] Department of Molecular Medicine and Biopharmaceutical Sciences, Graduate School of Convergence Science and Technology, College of Pharmacy, Seoul National University, Seoul, South Korea
[b] Biomedical Research Institute, Korea Institute of Science and Technology (KIST), Seoul, South Korea
[c] Research Institute of Pharmaceutical Sciences, College of Pharmacy, Seoul National University, Seoul, South Korea
[d] College of Pharmacy, Yeungnam University, Gyeongsan, South Korea
[e] Asan Medical Center, Department of Otolaryngology, College of Medicine, University of Ulsan, Seoul, South Korea
[f] College of Pharmacy, Chosun University, Gwangju, South Korea

ARTICLE INFO

Article history:
Received 11 July 2015
Received in revised form
27 January 2016
Accepted 27 January 2016
Available online 8 February 2016

Keywords:
TGF-β1
CXCL12
Polymeric bile acid
Low molecular weight heparin
Metastasis
Multi-stage targeting

ABSTRACT

Targeting multiple stages in metastatic breast cancer is one of the effective ways to inhibit metastatic progression. To target human metastatic breast cancer as well as improving patient compliance, we developed an orally active low molecular weight heparin (LMWH)-taurocholate conjugated with tetrameric deoxycholic acid, namely LHTD4, which followed by physical complexation with a synthetic bile acid enhancer, DCK. In breast cancer, both transforming growth factor-β1 (TGF-β1) and CXCL12 exhibit enhanced metastatic activity during the initiation and progression stages of breast cancer, thus we direct the focus on investigating the antimetastatic effect of LHTD4/DCK complex by targeting TGF-β1 and CXCL12. Computer simulation study and SPR analysis were performed for the binding confirmation of LHTD4 with TGF-β1 and CXCL12. We carried out *in vitro* phosphorylation assays of the consecutive receptors of TGF-β1 and CXCL12 (TGF-β1R1 and CXCR4, respectively). Effects of LHTD4 on *in vitro* cell migration (induced by TGF-β1) and chemotaxis (mediated by CXCL12) were investigated. The *in vivo* anti-metastatic effect of LHTD4 was evaluated in an accelerated metastasis model and an orthotopic MDA-MB-231 breast cancer model. The obtained K_D values of TGF-β1 and CXCL12 with LHTD4 were 0.85 and 0.019 μM respectively. The simulation study showed that binding affinities of LHTD4 fragment with either TGF-β1 or CXCL12 through additional electrostatic interaction was more stable than that of LMWH fragment. *In vitro* phosphorylation assays of TGF-β1R1 and CXCR4 showed that the effective inhibition of receptor phosphorylation was observed with the treatment of LHTD4. The expressions of epithelial to mesenchymal transition (EMT) marker proteins such as vimentin and Snail were prevented by LTHD4 treatment in *in vitro* studies with TGF-β1 treated MDA-MB-231 cells. Moreover, we observed that LHTD4 negatively regulated the functions of TGF-β1 and CXCL12 on migration and invasion of breast cancer cell. In several advanced orthotopic and experimental breast cancer metastasis murine models, the treatment with LHTD4 (5 mg/kg daily, p.o.) significantly inhibited metastasis compared to the control. Overall, LHTD4 exhibited anti-metastatic effects by inhibiting TGF-β1 and CXCL12, and the clinically relevant dose of orally active LHTD4 was found to be effective in preclinical studies without any apparent toxicity.

* Corresponding author. Department of Molecular Medicine and Biopharmaceutical Sciences, Graduate School of Convergence Science and Technology, College of Pharmacy, Seoul National University, 1 Gwanak-ro, Gwanak-gu, Seoul, 151-746, South Korea.
** Corresponding author. College of Pharmacy, Chosun University, 309 Pilmun-daero, Dong-gu, Gwangju, 501-759, South Korea.
E-mail addresses: srhwang@chosun.ac.kr (S.R. Hwang), yrbyun@snu.ac.kr (Y. Byun).

http://dx.doi.org/10.1016/j.biomaterials.2016.01.058
0142-9612/

1. Introduction

Breast cancer is one of the leading causes of cancer death among women as it tends to cause metastasis to distant organs, preferentially the bones, lungs and liver [1,2]. Despite significant improvements in early cancer detection and therapeutic interventions, prognosis for cancer patients with metastasis has not improved greatly [3,4]. Multiple factors are associated with the process of tumor colonization, in which tumor cells intravasate from the primary tumor site to the blood or lymphatic vessels and extravasate into distant organs [5]. Transforming growth factor β1 (TGF-β1), as one of the most closely associated factors, is responsible for the colonization of breast cancer cells from primary neoplasm to lung or other organs [6,7]. The TGF-β1 signaling controls a vast majority of cellular responses, including growth, differentiation, motility, and adhesion of tumor cells [8]. At the early stage of cancer, TGF-β1 acts as a tumor suppressor, but at the advanced cancer stage, it gets reprogrammed with tumor-promoting activities that include cancer migration, invasion, metastatic colonization, and evasion from immune attack as a prelude to distant dissemination [9,10]. Thus migration and invasion of epithelial carcinomas are highly influenced by TGF-β1, leading to a crosstalk between tumor stroma and breakdown of basement membrane, which is a molecular mechanism akin to epithelial-to-mesenchymal transitions (EMT) [11–13]. During EMT, carcinoma cells lose epithelial characteristics and acquire invasive properties.

Tumor cells establish a reverse transition from mesenchymal to epithelial (MET) morphology and re-acquire proliferative mechanisms to establish overt metastasis at a secondary site [14]. The chemokine receptor CXCR4, which is overexpressed in primary breast tumor cells, and its ligand CXCL12 are known to be associated with the MET process [14,15]. High levels of CXCR4 expression can direct chemotaxis and invasive responses to breast cancer cells and is correlated with poor clinical outcomes [16]. The binding of CXCL12 to CXCR4 promotes tumorigenic process of breast cancer cell by several mechanisms; 1) CXCR4-expressing cells are colonized to organs where CXCL12 is expressed, 2) elevated CXCL12 levels are associated with survival and growth of cancer cells, metastasis, and angiogenesis in a paracrine fashion [17,18]. For the treatment of metastatic breast cancer, several molecules targeting either TGF-β1 signaling or CXCR4–CXCL12 interaction had been developed [19]. However, considering the specific role of different molecular factors in the metastatic cascade, targeting a single factor would not be effective for blocking metastasis unless the same factor has an essential role in the later stage of the metastatic cascade [8].

Many studies have indicated that spontaneous and experimental metastasis could be efficiently inhibited by heparin, a well-known clinically established anticoagulant, primarily via its interaction with multiple factors and selectins [20]. The enormous structural diversity of heparin makes it possible to interact with and regulate the functions of wide range of proteins by binding to the heparin-binding domain (HBD) present in the structural features of the proteins [21]. The HBD consists of consensus sequences of proteins, patterns of clusters of basic and non-basic residues, and common spatial arrangements of basic amino acids [22]. Thus, we hypothesized that heparin or heparin-based single compound can simultaneously attenuate the functions of multiple factors at different stages of advanced metastatic breast cancer. However, in the light of therapeutic interventions, the use of unfractionated heparin or low molecular weight heparin (LMWH) is limited due to its high anticoagulant activity in blood and parenteral administration route.

Previously, we demonstrated that chemically modified heparins, developed by conjugating with different types of bile acids show high anti-angiogenic effects in tumor growth inhibition studies [23–27]. Among these modified heparins, taurocholate-conjugated LMWH (LHT7) had highly specific binding affinity to growth factors without any anticoagulant activity [23,28]. The increased binding affinity of LHT7 compared to LMWH was attributed to the presence of HBD in the growth factors and additional electrostatic interactions from the terminal sulfate groups of conjugated taurocholic acids. Thus, the presence of HBD in growth factors or cytokines and the binding stability of the heparin conjugates to those HBDs in different growth factors or cytokines help us to study and evaluate biological effectiveness of heparin conjugates, and targeting of their heparin moieties to growth factors and cytokines.

Here, we evaluated the therapeutic potential of orally active LHTD4, developed as a new oral anti-metastatic agent against advanced breast cancer metastasis. At first, LHTD4 was synthesized by conjugating LHT7, prepared as described in our previous studies, with a tetramer of dexoycholic acid [4]. LHTD4 and DCK (L-lysine-deoxycholylethylamine) were formulated; this ion-pairing complex masked the negative charge and increased the lipophilicity of LHTD4 [5]. Deoxycholic acid (DOCA) based enhancers have long been studied as an absorption enhancer for the oral delivery of negatively charged drugs [6]. Our LHTD4/DCK complex binds with the apical sodium-dependent bile acid transporters (ASBT) in the ileum and internalizes ASBT into the cytoplasm; a vesicular transport mechanism, where high-affinity binding of DOCA conjugates induces the functional transformation of ASBT in vesicles [7]. DCK augments the binding of LHTD4 with ASBT at the absorption site. Although LHTD4/DCK complexes were highly absorbed in the ileum, they were also absorbed in the duodenum. DCK improves the intestinal absorption of LHTD4 via targeting both enterocytes, each having a high ASBT expression (ileum) and a low ASBT expression (duodenum). Once the LHTD4/DCK complex enters the blood circulation, it dilutes and dissociates from each other due to reversible charge–charge interactions. Thus, DCK increases the oral bioavailability of LHTD4 without affecting the biological activity of LHTD4 itself. In this study, the potential of LHTD4 in a specific inhibition against TGF-β1 and CXCL12 was evaluated through their consensus sequence in heparin binding and additional interactions that could be governed by the conjugated bile acid moieties. Effects of LHTD4 on *in vitro* cell migration (induced by TGF-β1) and chemotaxis (mediated by CXCL12) were investigated. We also evaluated the *in vivo* therapeutic efficacy of LHTD4 in several advanced orthotopic and experimental breast cancer metastasis mouse models.

2. Materials and methods

2.1. Materials

LHT7 was synthesized by activating a 4-hydroxyl group of sodium taurocholate (TCA, Sigma–Aldrich, St. Louis, MO) with 4-nitrophenylchloroformate (Sigma–Aldrich) in the presence of triethylamine (Sigma–Aldrich), and introducing a primary amine into TCA via the addition of ethylenediamine (EDA, Sigma–Aldrich). The primary amine group introduced into TCA was conjugated with carboxyl group of LMWH (Fraxiparine®; GlaxoSmithKline, Brentford, UK) using 1-ethyl-3-(3-dimethylaminopropyl)-carbodiimide and *N*-hydroxysuccinimide (HOSu), resulting in LHT7. The product was analyzed by ^{1}H NMR (Avance, Bruker, MA), and the coupling ratio between LMWH and the conjugated TCA was determined by the previous procedure for the quantification of bile acids [23].

LHTD4 was synthesized by coupling LHT7 to a tetramer of deoxycholic acid (*tetra*DOCA) according to the previously described procedure [29,30]. In brief, for the synthesis of *tetra*DOCA, first,

lysine dimer BOC-CH_3O-lys(lys(boc)$_2$) was prepared by the peptide synthesis method. After the lysine dimer was activated using *N*,*N*′-dicyclohexylcarbodiimide (DCC, Sigma–Aldrich) and HOSu, the lysine trimer, BOC-CH_3O-lys(lys(boc)$_2$)$_2$, was obtained via the addition of 4-methylmorphorline. DOCA was activated using DCC and HOSu, and then four amine groups of the lysine trimer were reacted with the activated DOCA, thereby forming *tetra*DOCA. After the preparative purification on a silica gel-packed column, *tetra*-DOCA was reacted with EDA to obtain *N*-*tetra*deoxycholylethylamine (*tetra*DOCA-NH_2), followed by passing through a silica gel-packed column for the further purification [31,32]. Finally, LHT7 oxidized by potassium metaperiodate was reacted with *tetra*DOCA-NH_2, to obtain LHTD4.

Deoxycholylethylamine (DCK) was synthesized as described in the previous study, and used as an absorption enhancer [33]. A physical complex of LHTD4 and DCK was then prepared, also according to the previous study, by mixing in distilled water at a molar ratio of 1:10 (LHTD4:DCK). The formation of LHTD4/DCK complex was confirmed by turbidity measurement. The schematic structure of LHTD4/DCK complex is illustrated in Fig. 1.

2.2. Cell culture

Human breast adenocarcinoma MDA-MB-231 cells were purchased from the Korean Cell Line Bank (KCLB, Seoul, South Korea). The passage number of MDA-MB-231 used in experiments was 38–40. Luciferase-labeled MDA-MB-231 (MDA-MB231-LUC2, passage number 3–4) was purchased from Caliper Sciences, Inc. (Hopkinton, MA). Both types of MDA-MB-231 cell lines were cultured with Dulbecco's modified Eagle's media (high glucose) supplemented with 10% fetal bovine serum, 1% antibiotic–antimycotic, and 1% non-essential amino acid, and incubated at 37 °C in a CO_2 incubator.

2.3. Cell migration assay

The cell migration assay was carried out with MDA-MB-231 cell line using Oris™ Cell Migration Assay kit (Collagen I Coated, Platypus Technology, WI) according to the manufacturer's instruction. First, 1000 cells were seeded per well and incubated for 6 h in the CO_2 incubator. Then, after the removal of the stopper, the cells were again incubated overnight in the CO_2 incubator with the test materials. In one set of the experiments, the cells were treated with the vehicle control (growth factor-reduced media), TGF-β1 (10 ng/mL), LHTD4 (5 μg/mL) plus TGF-β1, and LMWH (5 μg/mL) plus TGF-β1, respectively. Another set of experiments was designed to evaluate the dose dependency of LHTD4 (with 10 ng/mL TGF-β1) at 50, 5, 0.5, 0.05 and 0.005 μg/mL. At the end, all cells were stained with Calcein-AM after the fixation of the cells with 4% PFA, and the migrated cells (in the middle of the well) were observed through fluorescence microscope (Nikon Co., Tokyo, Japan). All groups of cells were compared with the negative control group. All assays were carried out as triplicate for reducing the experimental error.

2.4. In vitro chemotaxis assay

The chemotaxis assays were carried out using Cytoselect™ 24-well cell migration assay kit (Cell Biolabs, Inc., San Diego, CA) with MDA-MB-231 cells as described in manufacturer's instruction. First, cells were seeded in the upper wells of the 24-well trans-migration chambers (pore size 8 μm), and the vehicle control (growth factor-reduced media), CXCL12 (100 ng/mL), CXCL12 plus LMWH (concentration was the same as other *in vitro* assays) and CXCL12 plus LHTD4 (concentration was the same as other *in vitro* assays) were added to the lower well, respectively. After an overnight incubation in the CO_2 incubator, all the plates were counted by staining the cells migrated to the lower chamber with the cell-stain solution (provided by the kit). The absorbance value of the extract with the cell-extraction solution (provided by the kit) was detected at 560 nm.

2.5. Binding kinetics of LHTD4 with TGF-β1

Binding affinity of LHTD4 to recombinant human TGF-β1 (R&D Systems, Minneapolis, MN) was measured on a surface plasmon resonance (SPR) system (BIAcore T100, GE Healthcare, Uppsala, Sweden). The analyte, LHTD4, was prepared at concentrations ranging from 0.001 to 1 mM in 10 mM EDTA, containing HEPES buffer supplemented with 150 mM NaCl, which was also used as a running buffer. To immobilize TGF-β1, the surface of a CM5 sensor chip (GE Healthcare, Uppsala, Sweden) was activated using the amine-coupling method. The immobilization of TGF-β1 was controlled to achieve 400–500 response units. The flow rate of the analyte was adjusted to 20 mL/min. To regenerate the surface of the sensor chip, 50 mM NaOH was discharged after each cycle of analysis. Each concentration ran in triplicate. The data were analyzed by curve fitting with BIAcore T100 evaluation software (GE Healthcare).

2.6. Molecular modeling of LHTD4 with TGF-β1 and CXCL12

The molecular structures of both TGF-β1 and CXCL12 have been reported [34,35]. The structure of LHTD4 fragment was created using ChemBioDraw Ultra 11.0 and ChemBio3D Ultra 11.0 (Cambridge Soft, CA). All bonds of LHTD4 fragment were treated as active torsional bonds. The 3D coordinates of both TGF-β1 and CXCL12 were converted into an appropriate format using the AutoDockTools package by adding Gasteiger charges. For all docking studies, grid boxes were centered at the heparin-binding domain of each protein. The molecular docking simulations of both TGF-β1 and CXCL12 were performed using the AutoDock Vina 1.0.3 program [36]. Illustrations of the 3D model were generated and visualized using the PyMol program.

2.7. TGF-β1 receptor I (TGF-β1R1) phosphorylation

In vitro TGF-β1R1 phosphorylation was evaluated both by immunoblotting and confocal imaging. For immunoblotting assay, MDA-MB-231 cells were seeded at 2×10^3 cells/well in 6-well plates. When the cells were 90–95% confluent, they were serum-starved overnight. The cells were then treated with the vehicle control (growth factor-reduced media), TGF-β1 (10 ng/mL), LHTD4 (5 μg/mL) plus TGF-β1, and LMWH (5 μg/mL) plus TGF-β1, respectively. The phosphorylation time was optimized at 3 h of the treatment. After incubation for 3 h, the cells were lysed using lysis buffer (20 mM Tris pH 7.4, 15% glycerol, 1% Triton X-100, 8 mM $MgSO_4$, 150 mM NaCl, phosphatase inhibitor and 1 mM EDTA in water), and the lysate was collected using a cell scraper after gently shaking on the orbital shaker. The supernatant of the lysate was collected after centrifugation (14,000 × *g* for 15 min) at 4 °C. The amount of protein present in the cell lysates was measured using a protein detection kit (Pierce, Rockford, Ill). For the western blot analysis, proteins were electrophoresed on a 12% Bis-Tris gel (Invitrogen, Carlsbad, CA).

For the visualization of phosphorylation in MDA-MB-231 cells, the cells were seeded in the confocal dish and cultured for 2 days. After an overnight starvation, the cells were treated with the vehicle control (growth factor-reduced media), TGF-β1 (10 ng/mL), LHTD4 (5 μg/mL) plus TGF-β1, and LMWH (5 μg/mL) plus TGF-β1 for 3 h, respectively. After washing, the cells were blocked with 4%

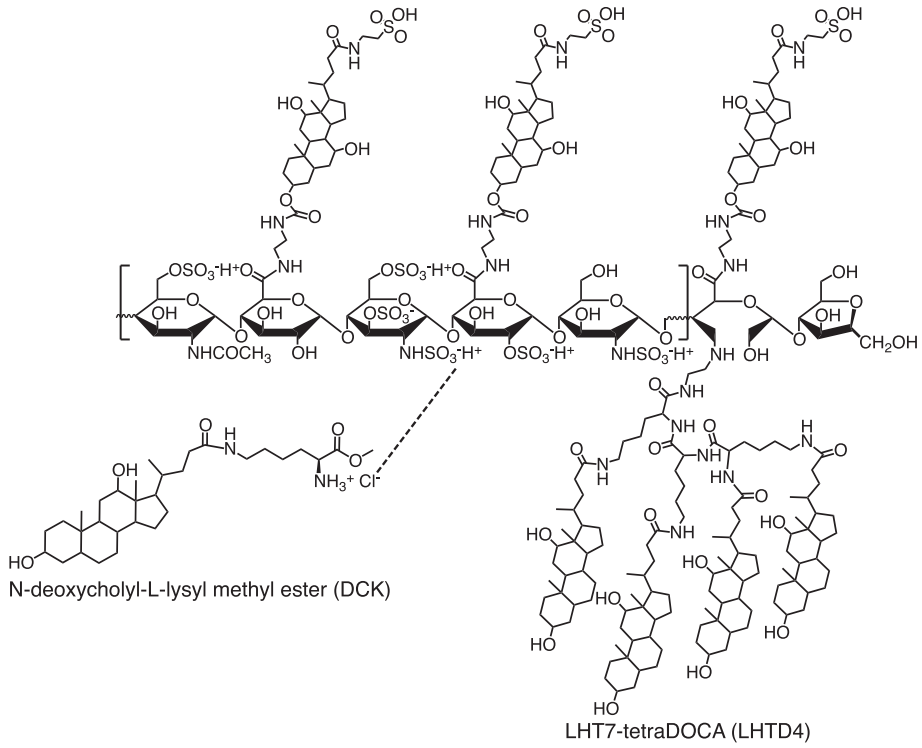

Fig. 1. The schematic structure of low molecular weight heparin-taurocholate-tetrameric deoxycholate (LHTD4) and N-deoxycholyl-L-lysine methyl ester (DCK) complex. Dashed line indicates the physical interaction between negatively charged sulfonyl groups of LHTD4 and positively charged lysine residues of DCK.

paraformaldehyde (PFA), then permeabilized using 3% Triton X-100 in a blocking solution containing 10% normal goat serum in PBS for 40 min. After permeabilization, the cells were incubated with human anti-goat TGFβ1R1 primary antibody (Abcam, Cambridge, UK) at 4 °C for overnight. The cells were washed and the primary antibodies were stained with Alexa Flour 488 (green)-labeled secondary antibody. Nuclei were counterstained with Hoechst 33258 dye (Sigma–Aldrich). Fluorescence images were then observed under a confocal microscope (Carl Zeiss LSM710, Leica DM IRB/E; Leica Co., Germany).

2.8. TGF-β1-induced epithelial–mesenchymal transition (EMT)

TGF-β1-induced EMT was investigated by evaluating the expression of vimentin and SNAIL-1. MDA-MB-231 cells were treated with vehicle control (growth factor-reduced media), TGF-β1 (10 ng/mL), LHTD4 (5 μg/mL) plus TGF-β1, and LMWH (5 μg/mL) plus TGF-β1, respectively. The expressions of vimentin and SNAIL-1 were confirmed using both immunoblotting and confocal imaging. Immunoblotting was performed as mentioned above, using anti-human vimentin antibody and anti-human SNAIL-1 antibody (R&D Systems Inc., Minneapolis, MN) with SDS-PAGE gels at the concentrations of 7.5%, 10% and 12%, respectively. Meanwhile, the human EMT 3-color immunocytochemistry kit (R&D Systems Inc., Minneapolis, MN) was also used for analysis of the expressions of vimentin and SNAIL-1 with the treatment of the vehicle control, TGF-β1 (10 ng/mL), LHTD4 (5 μg/mL) plus TGF-β1, and LMWH (5 μg/mL) plus TGF-β1, respectively. For this experiment, MDA-MB-231 cells were cultured until they were fully confluent. After 48 h incubation with the material, the cells were fixed with PBS containing 4% PFA, and blocked with PBS containing 10% normal donkey serum, 0.3% Triton® X-100, and 1% BSA. After blocking, the cells were incubated overnight at 4 °C in a blocking buffer with anti-human SNAIL-1 NL557-conjugated Goat IgG and anti-human vimentin NL493-conjugated Rat IgG from the kit; each of these were at a final concentration of 1× (1:10 dilution). Then the cells were washed, counterstained with Hoechst, and observed through confocal microscopy (Carl Zeiss LSM710, Leica DM IRB/E; Leica Co., Germany) using absorption at 557 nm and 493 nm for the expression of SNAIL-1 and vimentin, respectively, according to manufacturer's instruction. The experiment was repeated three times for each group for confirmation.

2.9. In vitro CXCR4 phosphorylation inhibition

CXCR4 phosphorylation was assessed using both immunoblotting and confocal imaging. For immunoblotting assay, MDA-MB-231 cells were cultured in 6-well dish at 2×10^3 cells/well. After the cells were 90–95% confluent, they were starved overnight. The following day, the cells were treated with the vehicle control (growth factor-reduced media), CXCL12 (100 ng/mL), CXCL12 plus LMWH (5 μg/mL) and CXCL12 plus LHTD4 (5 μg/mL) for 3 h, respectively, and subjected to lysis using lysis buffer (20 mM Tris pH 7.4, 15% glycerol, 1% Triton X-100, 8 mM $MgSO_4$, 150 mM NaCl, phosphatase inhibitor and 1 mM EDTA in water). The lysate was collected using a cell scraper after gently shaking in an orbital shaker, and then the supernatant of the lysate was collected after centrifugation (14,000 × *g*, for 15 min) at 4 °C. The amount of protein present in the cell lysates was measured using a protein detection kit (Pierce, Rockford, Ill). The western blot was performed using 10% SDS-PAGE.

For the visualization of CXCR4 phosphorylation in MDA-MB-231 cell lines, the cells were seeded into the IVF confocal dish and cultured for 2 days. After an overnight starvation, the cells were treated with the vehicle control (growth factor-reduced media), CXCL12 (100 ng/mL), CXCL12 plus LMWH (5 μg/mL), and CXCL12 plus LHTD4 (5 μg/mL) for 3 h, respectively. The cells were washed, fixed with 4% PFA, and permeabilized using 3% Triton X-100 in a

blocking solution containing 10% normal goat serum in PBS for 40 min. After permeabilization, the cells were incubated with human anti-rabbit CXCR4 primary antibody (Abcam, Cambridge, UK) at 4 °C for overnight. The cells were washed and the primary antibodies were stained with Alexa Flour®488 (green)-labeled secondary antibody. Nuclei were counterstained with Hoechst 33258 dye. Fluorescence images were then observed under a confocal microscope (Carl Zeiss LSM710, Leica DM IRB/E; Leica Co., Germany).

2.10. In vivo orthotopic breast cancer model

Murine breast cancer cell line, 4T1-Luc-tdTomato was purchased from Cell Biolab Inc. (San Diego, CA) and used as *in vivo* orthotopic model for the evaluation of LHTD4/DCK complex (Supplementary Fig. S4A). After this evaluation, we finally applied our drug on the human metastatic breast cancer orthotopic model. For this, orthotopic implantation of MDA-MB-231-LUC2 cells (2×10^5 cells) was performed through injection into the mammary fat pad of 4- to 6-week-old female SCID (CB-17) mice. When the volume of the tumor reached approximately 200 mm^3 (10^5 photons/s), all of the mice were divided into two groups (the control and the LHTD4/DCK treatment (5 mg/kg daily, p.o.) groups), and then the treatment started. Every 7th day after the treatment, mice were imaged using the IVIS-Xenogen 100 (Caliper Life Sciences) at 10 min after the i.p. injection of D-luciferin (Parenkeimer, NY) at 150 mg/kg dose (37.5 mg/mL per mice), and the metastatic spread was evaluated through the image analysis using the Live Imaging 4.2 (Parenkeimer). The mice were sacrificed 4 weeks after the treatment when more than 50% of the group reached an average tumor volume above 1500 mm^3.

2.11. In vivo experimental metastasis model

For the evaluation of LHTD4/DCK complex in the later stage of metastasis, first, we evaluated its efficacy on murine breast cancer cell line in a 4T1-Luc-tdTomato tumor resection model (Supplementary Fig. S5A). Next, in a different set of experiment, we evaluated the LHTD4/DCK's effect in the human experimental metastatic breast cancer model. For this, MDA-MB231-LUC2 (1.3×10^6 cells) were injected directly into the tail vein of 6- to 8-week-old female BALB/c allogeneic athymic nude (*nu*/*nu*) mice (Orient Bio Inc., Gyungi-do, Korea). The mice were randomly divided into two different groups, the control and LHTD4/DCK at a dose of 5 mg/kg daily, p.o., n = 10 in each group. Metastatic disease progression in MDA-MD-231 tumor-bearing mice was monitored weekly. For this model, mice were treated for 60 days and imaged using the IVIS-Xenogen 100 (Caliper Life Sciences) at 10 min after the injection of D-luciferin. The luciferase activity was measured using the same protocol as mentioned in the previous metastasis model. Images were analyzed using Live Imaging® software and normalized against the control (non-treated group). All of the mice were sacrificed at 60th day of tumor inoculation. The images of the post-dissected organs were observed by inducing Luciferin activity as the following: after injection of D-luciferin, the organs were collected within 5 min, and then the images were captured within 6 min.

3. Results

3.1. Binding analysis of LHTD4 to TGF-β1

Fragment-based structural studies were used to confirm whether LMWH and LHTD4 could be bound to TGF-β1. We performed a molecular docking modeling with the X-ray crystal structure of TGF-β1 and fragments of LMWH and LHTD4. The model structure of the TGF-β1/LHTD4 complex showed that Arg 25, Lys 31, Lys 37, Tyr 91 and His 34 of TGF-β1 played critical roles in the binding to LHTD4 fragment (Supplementary Fig. S1A). In concurrence with the binding mode of LMWH to TGF-β1, the key interactions of the main chain of LHTD4 were observed with the heparin binding sites in TGF-β1 (Supplementary Fig. S2A). In addition, electrostatic interactions with Lys 26 of TGF-β1 and hydrophobic interactions with Phe 30 and Phe 32 of TGF-β1 were observed with the terminal sulfate group and the sterane core of the conjugated taurocholate moiety of LHTD4, respectively.

To gain further insight into the interactions between LMWH or LHTD4 and TGF-β1, we measured the dissociation rate constants at equilibrium (K_D) using SPR. The K_D values for full-length LMWH and LHTD4 to recombinant TGF-β1 were 5.1 and 0.85 μM, respectively (Fig. 2A). Binding affinity measurements along with the molecular docking studies substantiated the notion that the additional favorable interactions between the conjugated taurocholate moieties of LHTD4 and TGF-β1 could cooperatively stabilize the complex structure to increase the binding affinity.

3.2. Inhibition effect of LHTD4 on TGF-β1 mediated signaling and EMT in breast cancer cells

To investigate the role of TGF-β1 binding, we first examined the inhibition effects of LMWH and LHTD4 on the TGF-β1 induced TGF-β1R1 phosphorylation in the MDA-MB-231 breast cancer cell line. TGF-β1 strongly stimulated the phosphorylation of TGF-β1R1, whereas both LMWH and LHTD4 inhibited the TGF-β1 mediated TGF-β1R1 phosphorylation in a dose-dependent manner in MDA-MB-231 cancer cells; in addition, LHTD4 showed better inhibition efficacy than LMWH (Fig. 3A–C). To investigate the potential role of LHTD4 in TGF-β1-mediated changes in EMT transition, TGF-β1-induced expression and cellular distribution of EMT markers were examined by western blot and immunofluorescence staining in MDA-MB-231 cells. Since MDA-MB-231 cells do not generally express E-cadherin, the expressions of vimentin and SNAIL-1 except E-cadherin were evaluated in this study. The expressions of vimentin and SNAIL-1 induced by TGF-β1 were decreased in the presence of LHTD4 (Fig. 3D). Immunofluorescence analysis showed

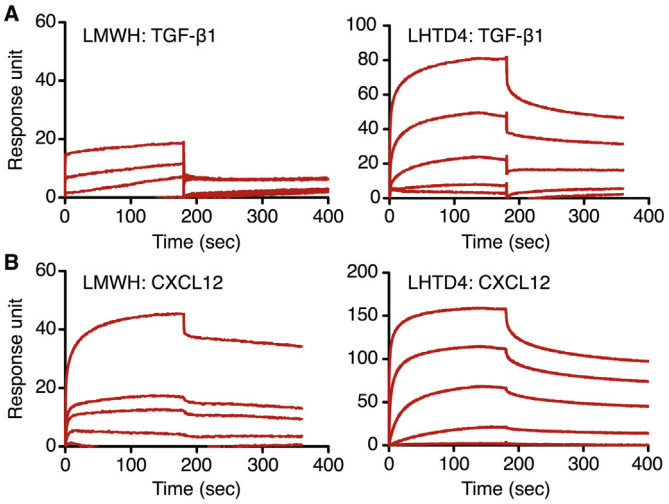

Fig. 2. Surface plasmon resonance (SPR) binding affinity study between LMWH or LHTD4 and TGF-β1 or CXCL12. (A) SPR analysis between LMWH-TGF-β1 (left) and LHTD4-TGF-β1 (right). (B) SPR analysis between LMWH-CXCL12 (left) and LHTD4-CXCL12 (right). Dissociation rate constants are calculated from the response curves at the concentrations ranging from 0.001 to 100 μM.

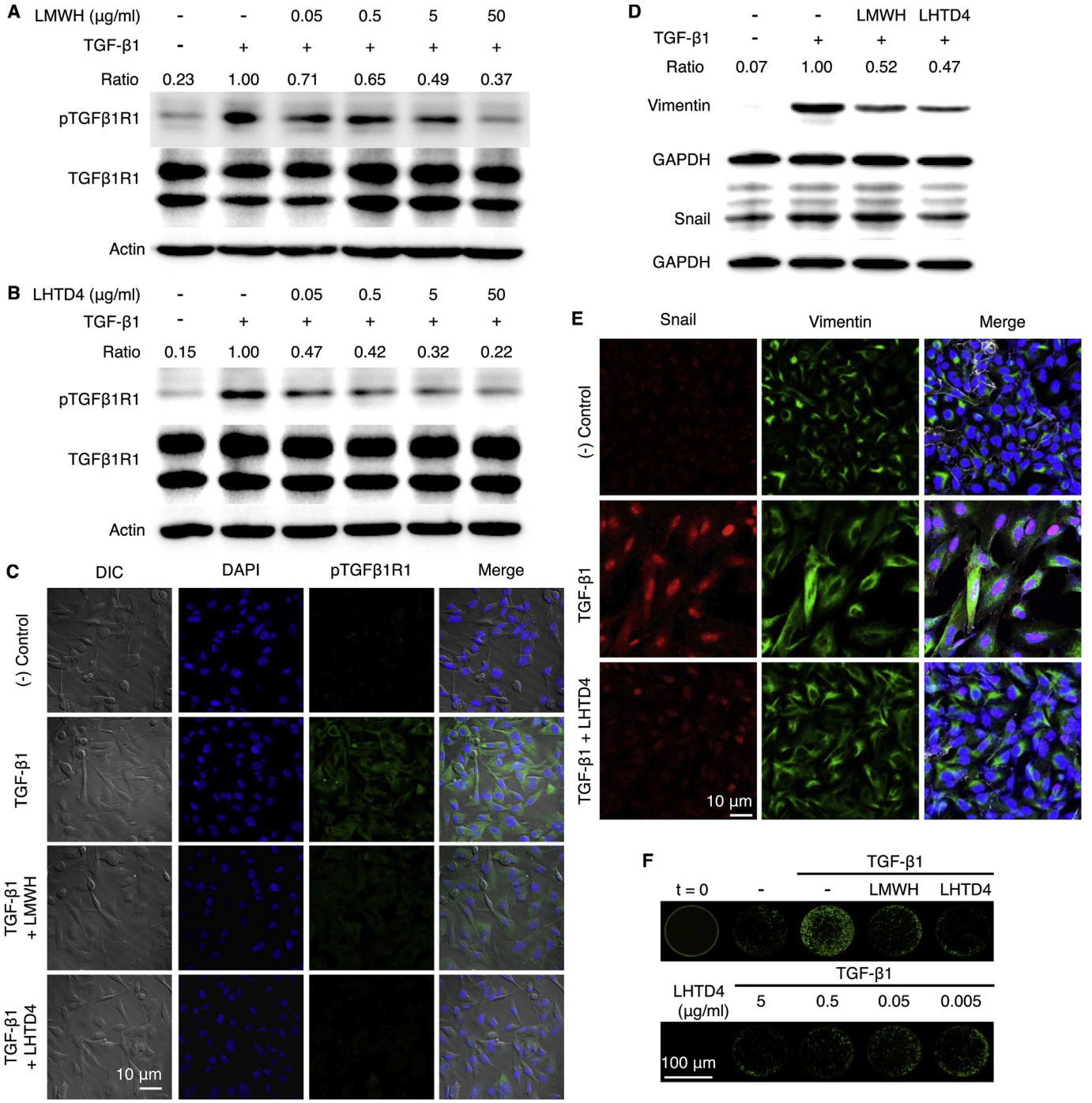

Fig. 3. *In vitro* TGF-β1 inhibition study. The TGFβ1R1 receptor phosphorylation inhibition by (A) LMWH and (B) LHTD4 with the ratio of the intensity of test samples dividing by the intensity of internal reference. (C) The confocal images of the TGFβ1R1 receptor phosphorylation by both LHTD4 and LMWH. Immunoblotting (D) and confocal images (E) of epithelial to mesenchymal transition (EMT) markers when cells were treated with LHTD4 in the presence of TGF-β1. (F) Cell migration assay induced by TGF-β1 with the treatment of LHTD4 and LMWH (upper row), migratory inhibition of LHTD4 at different concentrations (lower row).

that TGF-β1 inhibition by LHTD4 suppressed the nuclear expression of SNAIL-1 and vimentin filament network in MDA-MB-231 cells (Fig. 3E). These results suggest that LHTD4 plays an important role in suppressing TGF-β1-induced metastasis initiation.

Next, we investigated the migration inhibition effect of LHTD4 on MDA-MB-231 cells in the presence of TGFβ. LHTD4 effectively inhibited TGF-β1-induced cell migration. In another set of experiments, we observed that it exhibited inhibitory effect in a dose-dependent manner (Fig. 3F). These results indicated that LHTD4 inhibited the cell migration by blocking the TGF-β1 signaling pathway.

3.3. Inhibition effect of LHTD4 on CXCL12-mediated signaling and breast cancer cell invasion

The migration and successful seeding of breast cancer cells to other organs is typically guided by CXCL12 and its receptor CXCR4, which can direct chemotaxis and invasive responses. Heparin can

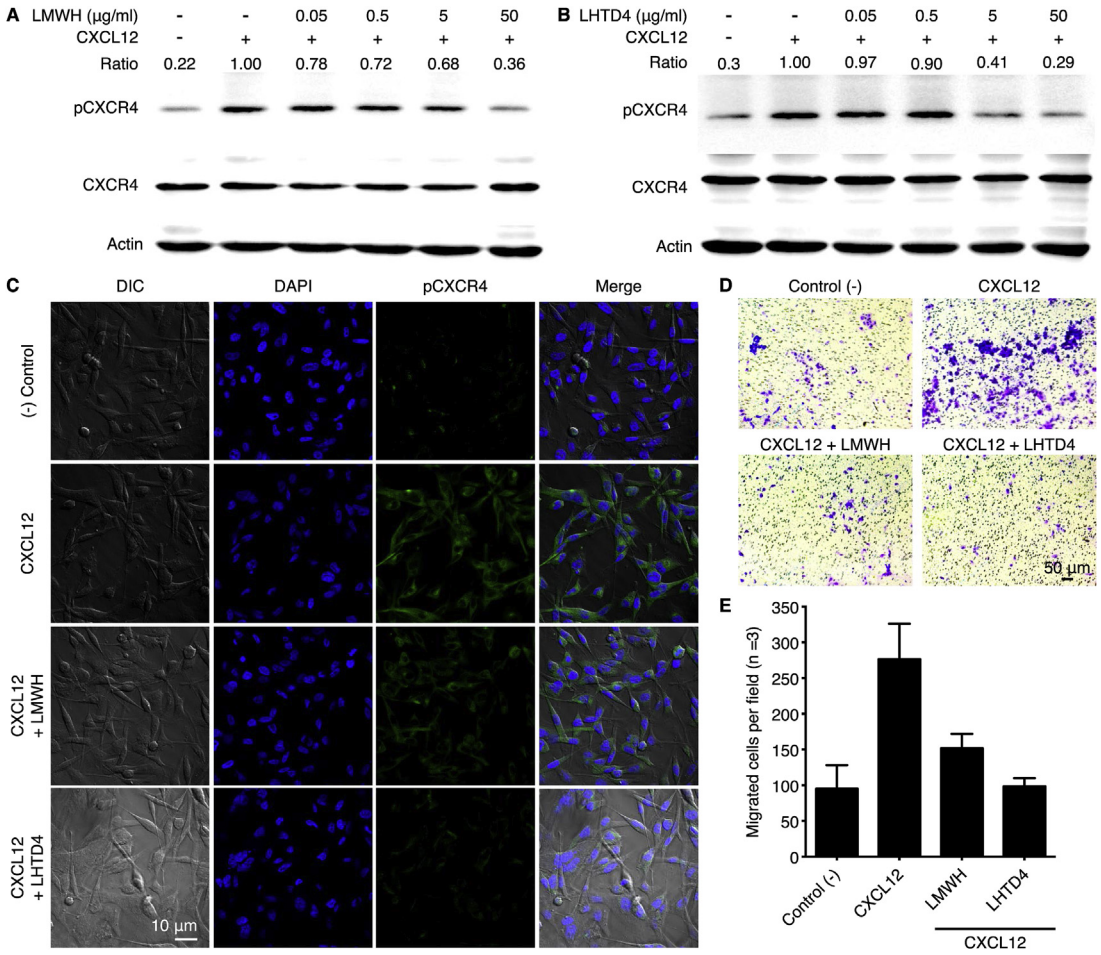

Fig. 4. *In vitro* CXCL12 inhibition study. The evaluation of inhibitory effect on the phosphorylation of CXCL12 receptor, CXCR4, by (A) LMWH and (B) LHTD4 through immuno blotting with the ratio of the intensity of test sample dividing by the intensity of internal reference. (C) The evaluation of inhibitory effect on the phosphorylation of CXCL12 receptor, CXCR4, by LMWH and LHTD4 through confocal imaging. (D) The chemotaxis inhibition assay with the MDA-MB-231 cells induced by CXCL12 with LHTD4 and LMWH. (E) Quantitative analysis for the chemotaxis inhibition with the MDA-MB-231 cells induced by CXCL12 by LHTD4 and LMWH.

be bound to the chemokine CXCL12 through its HBD and block CXCL12/CXCR4 signaling. Therefore, we hypothesized that LHTD4 could also modulate the CXCL12/CXCR4 signaling pathway in breast cancer and block the function of CXCL12/CXCR4 pathway in tumor metastasis. Previous studies demonstrated that the binding sites of CXCL12 to heparin were Lys 24, His 25, Lys 27, and Arg 41 of the six-stranded β-sheet of CXCL12 dimer [37]. The molecular docking of LHTD4 fragment with the HBD of CXCL12 showed that the saccharide chain of LHTD4 fragment was located near the cluster of residues mentioned above and there would be potential peripheral involvement of taurocholate moiety of LHTD4 with Phe 13 and Phe 14 residues of CXCL12 (Supplementary Figs. S1B and S2B). To directly assess the effect of taurocholate conjugation on the binding with CXCL12, we measured binding affinity of immobilized CXCL12 using SPR. Fig. 2B illustrates the changes in binding responses as a function of concentrations of LMWH and LHTD4 that were used to calculate the K_D values. LMWH exhibited a K_D value of 1.9 μM whereas LHTD4 had 100 times higher binding affinity with a lower K_D value of 0.019 μM.

We also investigated the effect of LHTD4 on CXCL12/CXCR4 signaling pathway. CXCL12 strongly phosphorylated its receptor CXCR4 after stimulation for 3 h, whereas LHTD4 blocked CXCL12-induced CXCR4 phosphorylation in a dose-dependent manner in MDA-MB-231 cells (Fig. 4A–C). LHTD4 showed better inhibition of CXCL12/CXCR4 signaling than LMWH due to its higher binding affinity with CXCL12 (Fig. 4B). CXCL12-induced chemotaxis in breast cancer cells (190.8% ± 30.3%, $p = 0.006$ vs. control) was completely blocked by LHTD4 (Fig. 4D and E). Quantification of the invasive breast cancer cells showed 45.1% ± 4.2% ($p = 0.01$ vs. CXCL12) and 64.4% ± 2.4% ($p = 0.003$ vs. CXCL12) inhibition by LMWH and LHTD4, respectively (Fig. 4E). Taken together, all our data suggest that LHTD4 inhibits CXCR4 receptor ligation and CXCL12-induced chemotaxis in breast cancer cell line.

3.4. LHTD4 inhibits metastases in the 4T1 orthotopic mammary carcinoma model

To evaluate the therapeutic potential of LHTD4 *in vivo*, we investigated whether LHTD4 could inhibit metastases in the murine 4T1 breast cancer model. Firstly, in the orthotopic mammary carcinoma model, $4T1^{Luc+}$ cells were metastasized to the lung, bones and liver in the control mice at 3 weeks of the primary tumor development (Supplementary Fig. S3). Bioluminescence imaging of the whole body and excised organs confirmed a significantly decreased rate of metastasis in LHTD4 treatment group as compared to the positive control (Supplementary Fig. S3B). Reduced luciferase units in the lungs, with representative hematoxylin and eosin (H&E) staining, were indicative of decreased tumor burden in the mice treated with LHTD4 (Supplementary Fig. S3C).

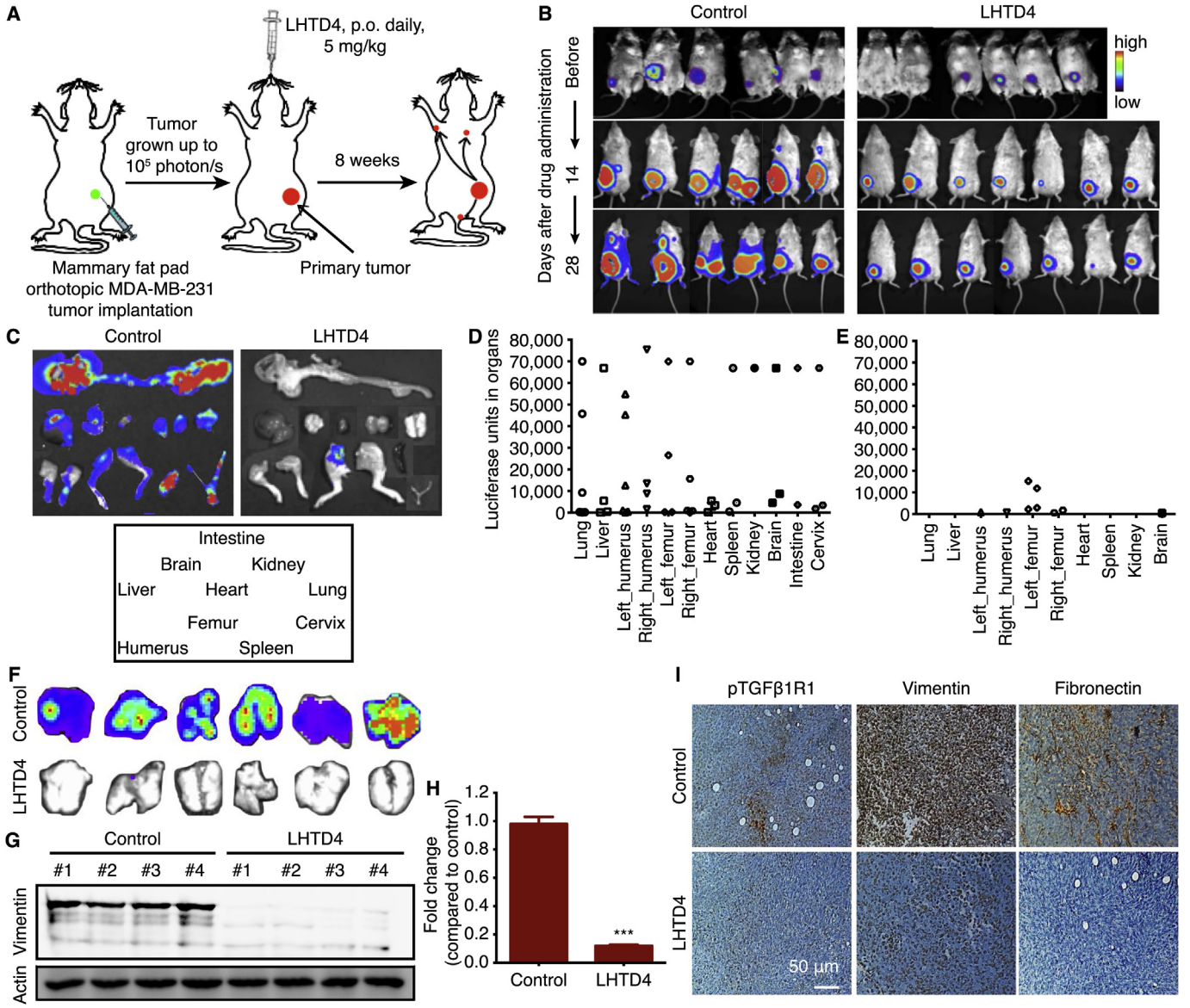

Fig. 5. The anti-metastatic effect of LHTD4 in murine orthotopic metastatic breast cancer model. (A) MDA-MB-231^{Luc+} cells were implanted into the mammary fat pad of SCID mice and treated with vehicle (control) or LHTD4 (5 mg/kg daily) for 8 weeks, after tumors reached 200 mm^3 in size (corresponding to bioluminescence values of 10^5 photons/s). (B) Bioluminescence imaging for observation of tumor growth delay and inhibition of metastasis after long-term LHTD4 treatment compared to control group. (C) At the end of the experiment, multiple organs including the lung, liver, bone, heart, spleen, kidney, brain, intestine, and cervix were dissected and luciferase activity was assayed as a proxy for spread of tumor cells. Luciferase activity in multiple organs from (D) control group and (E) LHTD4 treatment group. (F) Representative bioluminescence imaging of isolated whole lungs showing the number of nodules in the lungs of control and LHTD4 treated mice. The analysis (G) and quantitation (H) of vimentin expression in tumors as observed by western blot. *** indicates $p < 0.001$ vs control tumor. (I) TGFβ1R1 phosphorylation and the expression of vimentin and fibronectin as observed by immunohistochemistry analysis.

We next evaluated the effect of short-term LHTD4 treatment (5 mg/kg daily for 2 weeks) on spontaneous metastases to distant organs generated after surgical removal of primary tumor using the protocol illustrated in Supplementary Fig. S4A. Surgical resection of orthotopically grown 4T1^{Luc+} tumors led to spontaneous metastasis in almost every organ including the lung, spleen, kidney, bone, cervix, brain, and intestine in the control group (Supplementary Fig. S4B). On the contrary, mice that received short-term LHTD4 treatment showed a significant decrease in metastatic tumor burden as measured by bioluminescence imaging. Corresponding luciferase activity curves show a dramatic decrease of the mean values in LHTD4-treated group as compared to control group (Supplementary Fig. S4C), suggesting that LHTD4 could inhibit spontaneous metastasis of highly invasive mammary carcinoma at 5 mg/kg concentration.

3.5. LHTD4 inhibits metastasis in the MDA-MB-231 orthotopic xenograft model

With positive results from the short-term treatment of LHTD4, the effect of long-term LHTD4 treatment was investigated in the MDA-MB-231 orthotopic xenograft model. MDA-MB-231^{Luc+} cells were implanted into the mammary fat pad of SCID mice and treated with the vehicle (control) or LHTD4 (5 mg/kg daily) for 8 weeks after the tumor size reached 200 mm^3 (corresponding to bioluminescence values of 10^5 photons/s) (Fig. 5A). Both significant tumor growth delay and the inhibition of metastasis were observed in the long-term LHTD4 treatment group but not in the control group (Fig. 5B). At the end of the experiment, the organs were dissected and the luciferase activity was assayed as a proxy for spread of tumor cells. Increased overall metastatic tumor burden was found

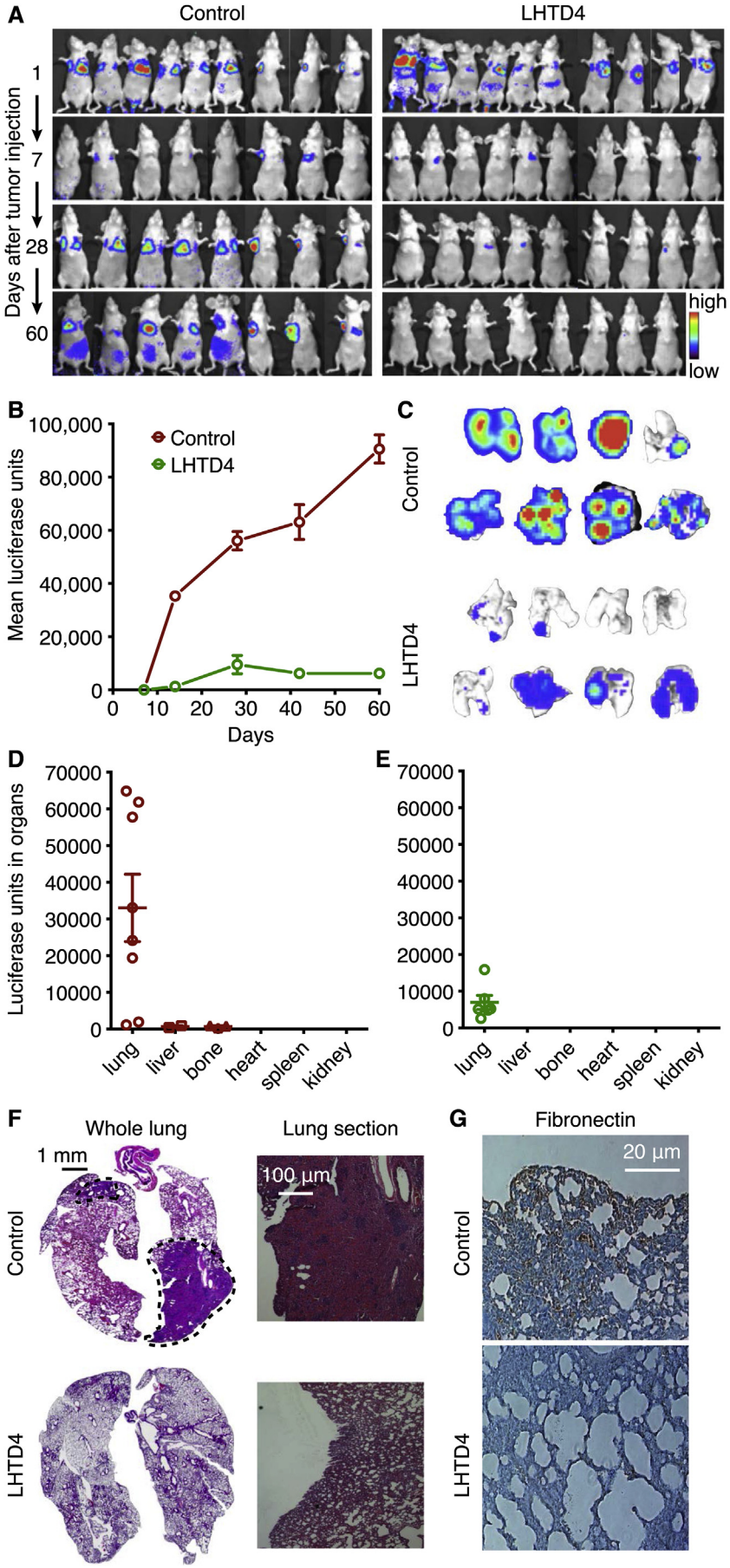
A
Control
LHTD4
Days after tumor injection
1
7
28
60
high
low
B
Mean luciferase units
100,000
80,000
60,000
40,000
20,000
0
Control
LHTD4
0 10 20 30 40 50 60
Days
C
Control
LHTD4
D
Luciferase units in organs
70000
60000
50000
40000
30000
20000
10000
0
lung liver bone heart spleen kidney
E
70000
60000
50000
40000
30000
20000
10000
0
lung liver bone heart spleen kidney
F
Whole lung
Lung section
1 mm
100 μm
Control
LHTD4
G
Fibronectin
20 μm
Control
LHTD4

in the control mice in multiple organs including the lung, liver, bones, heart, spleen, kidney, brain, intestine, and cervix (Fig. 5C). On the other hand, the long-term LHTD4 treatment group showed a significant decrease in metastatic tumor burden in most of the organs except the bones. In addition, the total tumor burden and the luciferase activity were significantly lower in the LHTD4 treatment group than in the control group (Fig. 5D and E). The lungs were removed and the tumor nodules per lung were counted. Bioluminescence imaging of the whole lungs confirmed that the lungs of the LHTD4-treated mice had virtually no nodules or tumors (Fig. 5F). Furthermore, the LHTD4-treated mice did not show any changes in the body weight compared to the control mice (data not shown), suggesting that LHTD4 did not cause any apparent toxicity *in vivo*.

To confirm the mechanism by which LHTD4 inhibited tumor metastasis, we evaluated the involvement with metastasis-related TGF-β1 signaling pathways in tumors from the control and the LHTD4-treated mice. LHTD4 reduced the phosphorylation of TGF-β1R1 and the expressions of vimentin and fibronectin, as observed by western blot and an immunohistochemistry analysis (Fig. 5G–I). These results demonstrated that LHTD4 suppressed breast cancer metastasis by blocking TGF-β1 signaling pathways.

3.6. Prevention effect of LHTD4 on experimental lung metastasis of MDA-MB-231 human breast cancer in vivo

Human metastatic breast cancer MDA-MB-231^{Luc+} cells were injected into the tail vein of nu/nu mice. LHTD4 was orally administered for 60 days at a dose of 5 mg/kg/day, and the prevention effect was proven by bioluminescence imaging to check the metastatic spread to the lungs and other organs (Fig. 6A). MDA-MB-231^{Luc+} cells that were injected into the tail vein were localized in the lungs, and orally administered LHTD4 almost completely blocked the development of lung metastasis. As demonstrated by the total photon flux, the effect was sustained over a period of 60 days until the experiment was terminated (Fig. 6B). MDA-MB-231^{Luc+} cells injected in the control mice tended to metastasize preferentially in the lungs and then in the liver and bones, and all of the mice in the control group showed high incidences of metastasis to the lungs (Fig. 6C and D). On the other hand, the LHTD4-treated group showed a minimal incidence of metastasis only in the lungs, without any detectable metastasis in other organs (Fig. 6C and E). The photon flux in the lungs was significantly reduced (84.0% ± 5.4%, $p = 0.01$) for the LHTD4 as compared to the control mice (Fig. 6D). H&E staining of the whole lungs and lung sections confirmed that there were significantly lower or almost no metastatic areas in the lungs of the LHTD4-treated mice than in those of the control mice (Fig. 6F).

Since the mobilization of CXCR4 positive breast cancer cells to the host lungs that secrete CXCL12 may facilitate an enhanced "pre-metastatic niche", we evaluated whether blocking the CXCL12/CXCR4 signaling would be involved in the anti-metastatic effect of LHTD4. Immunohistochemical staining for MDA-MB-231^{Luc+} tumor tissue in mouse lungs was performed using anti-human antibody for fibronectin (Fig. 6G). Increased fibronectin expression in metastasized breast cancer cells indicated the increase of micrometastasis in the lungs of the control mice, which corresponded to activation of CXCL12/CXCR4 signaling. Contrastively, fibronectin expression was not observed at all in the lungs of LHTD4-treated mice, suggesting that LHTD4 could inhibit breast cancer metastasis by altering the CXCL12/CXCR4 signaling in distant organs.

4. Discussion

LHTD4, a chemical conjugate of LHT7 and tetramer of deoxycholic acid, was synthesized to overcome the poor bioavailability and short half-life of LHT7. The efficacy of LHTD4 was similar to that of LHT7 in terms of inhibiting VEGF activity *in vitro* and anti-angiogenesis activity in a tumor model of squamous cell carcinoma (SCC7) *in vivo*. The anti-angiogenic effect of LHTD4 might use completely different mechanisms besides its anti-angiogenic effect in different metastasis experimental settings in this study. Thus, in this study, we sought to apply the LHTD4 by exploiting its anti-metastatic properties. TGF-β1 and CXCL12 both have been proven to play most critical roles in the metastatic progression of breast cancer cells regarding EMT progression and seeding to distant organs, respectively. Therefore, in this study, we report a new therapeutical function of LHTD4, focusing on tumoral metastasis. Since TGF-β1 modulates metastasis progression via EMT, the treatment of many types of cancers, including breast cancer, can be associated with blocking the TGF-β1 signaling pathway. Moreover, the CXCR4 receptor is up regulated in the primary breast cancers than that of normal breast cells, whereas relatively high levels of RNA expression for CXCL12 ligand are observed in the common metastatic sites of breast cancer. Focusing on the metastasis promotion and initiation of colonization in human breast cancer cells, we applied the orally active low molecular weight heparin triple conjugate, LHTD4. Since TGF-β1 modulates metastasis progression via EMT, the treatment of many types of cancers, including breast cancer, can be associated with blocking the TGF-β1 signaling pathway. Moreover, the CXCR4 receptor is regulated more in the primary breast cancer cells than in the normal breast cells whereas relatively high levels of RNA expression for CXCL12 ligand are observed in the common metastatic sites of breast cancer [38,39]. When we evaluated the binding affinity of the LHTD4 with TGF-β1 and CXCL12 using computational molecular dynamics and SPR analysis, LHTD4 showed higher binding affinity than the LMWH fragment. The LHTD4 fragment was bound to the cytokine TGF-β1 through HBD. Sulfate groups of the heparin fragment (degree of polymerization (dp) = 4) can interact with the HBD of TGF-β1 by charge-to-charge interactions. In addition, sulfate group of taurocholate moiety of LHTD4 enhanced the binding affinity of LHTD4 to the HBD. It was reported that glycosaminoglycan fragments could bind with several cytokines and growth factors and thus play an important role in the maintenance of stable cytokine gradients required to direct cell migration and the protection of cytokines from proteolytic degradation [40].

The evaluation of TGF-β1-induced TGF-β1R1 phosphorylation in the MDA-MB-231 breast cancer cell line showed that LHTD4 inhibited the TGF-β1-mediated TGF-β1R1 phosphorylation, indicating a decreased receptor activation. In the TGF-β1-mediated signaling, TGF-β1 is bound to TGF-β1R2, and then the phosphorylation of TGF-β1R2 leads to the phosphorylation of the next

Fig. 6. The anti-metastatic effect of LHTD4 in murine accelerated metastatic model. (A) Human metastatic breast cancer MDA-MB-231^{Luc+} cells were injected into the tail vein of nu/nu mice. LHTD4 was orally administered for 60 days at a dose of 5 mg/kg/day, and the preventive effect was proven by bioluminescence imaging to check the metastatic spread to lung and other organs. Treatment was initiated at 24 h after tail vein injection in order to exclude any potential direct drug effect on tumor cells. (B) The total photon flux over a period of 60 days in the lungs of mice. (C) Bioluminescence imaging of isolated whole lungs showing the number of nodules in the lungs of control and LHTD4 treated mice. At the end of the experiment, multiple organs including the lung, liver, bone, heart, spleen, kidney, brain, intestine, and cervix were dissected and luciferase activity was assayed as a proxy for spread of tumor cells in both (D) control group and (E) LHTD4 treatment group. (F) H&E staining showing tumor metastasis in the whole lungs and lung sections at higher magnifications in the control and LHTD4-treated group. Metastatic regions are marked as dashed line. (G) Immunohistochemical staining for MDA-MB-231^{Luc+} tumor tissue in mouse lungs was performed using anti-human antibody for fibronectin.

consecutive receptor TGF-β1R1. Transcription factors including SNAIL-1 are then activated, which help to up-regulate several mesenchymal markers such as vimentin and N-cadherin. Moreover, the activation of TGF-β1 signaling also down-regulates the epithelial markers, such as E-cadherin, syndecan and laminin-1. Thus, the actin formation and the loss of the junctional proteins in cancer cells initiate metastasis and the loss of adhesive property between cells leads to cell migration.

Sometimes, the activation of the transcription factors can be followed by non-SMAD-dependent pathway for the initiation of TGF-β1-dependent EMT. Through immunoblot analysis and confocal imaging, we found that MDA-MB-231 cells, treated with the LHTD4, show inhibition of TGF-β1R1 phosphorylation, which eventually decreases the expression of mesenchymal marker, vimentin. On the other hand, in the orthotopic breast cancer model, LHTD4 treatment showed reduction in metastatic events. Histological and immunoblotting analyses of the tumor tissue showed decreased TGF-β1R1 phosphorylation and decreased expression of mesenchymal markers, such as vimentin and fibronectin. All of these findings suggest that blocking of TGF-β1 by LHTD4 can prevent metastasis.

Meanwhile, the targeting of CXCL12 by heparin has shifted the monomer–dimer equilibrium to dimerization [41]. Moreover, Clore and co-workers found that the pocket formed by LYS24, His25, Ala40, Arg41, Gln48, and Tyr61 of CXCL12 interacts with a CXCR4 peptide [42]. Since the binding pocket of CXCL12 with CXCR4 overlaps with the part of HBD in CXCL12, it was hypothesized that the CXCR4 and heparin moieties would show some competitive binding to the CXCL12 [43]. The antagonism of heparin moieties is helpful in preventing the “seeding” of cancer cells in the distant organs, which are rich in CXCL12. When we simulated binding of the taurocholate-conjugated dp4 LHTD4 moiety with the CXCL12 dimer, we found that the binding became more stable due to electrostatic binding of the extra sulfonate groups in the taurocholate moiety with positively charged amino acids present in the HBD of CXCL12. In the chemotaxis assay, LHTD4 inhibited the chemotaxis induced by CXCL12. Moreover, LHTD4 could more effectively inhibit the phosphorylation of CXCR4 than LMWH. All of these results indicate that the stable binding of LHTD4 with CXCL12 could inhibit the activation of the CXCL12–CXCR4 pathway owing to the competitive binding with CXCR4 receptor. Finally, in the accelerated metastasis model, where the effect of the primary tumor microenvironment (the effect of TGF-β1) was absent, the development of nodules in the lungs was inhibited by LHTD4 as confirmed by the histological evaluation.

5. Conclusion

Targeting metastasis by a single molecule could be imperfect because the involvement of different pathways and several consecutive steps are responsible for the rise of resistance to the anti-metastatic therapy. Thus, our study was designed to focus on targeting both primary metastasis stage and the secondary development stage of the metastasis (Seeding stage) with a formulation developed for patient compliance. We reported that the oral formulation of LHTD4/DCK complex could be a good choice for the treatment of metastatic breast cancer as it can target multiple pathways of metastasis. LHTD4 primarily showed anti-metastatic effects via blocking of TGF-β and CXCR4 signaling pathway at different stages of metastasis progress. However, it is hard to say that LHTD4 only targets TGF-β1 and CXCL12–CXCR4 pathways since many other proteins also have heparin-binding domain. Regarding the inhibition of heparanase activity, selectins, tissue factor pathway inhibitors, leukocyte recruitment, and tumor cell–platelet interactions, some studies have correlated the non-anticoagulant function of heparin with cancer metastasis [44]. Many other heparin-binding factors have their own relative functions with the breast cancer progression and metastasis that include, but not limited to, fibroblast growth factors, hepatocyte growth factors, bone morphogenic proteins, Wnt-Hedgehog pathway, fibronectin, collagen, etc. [45]. A polyanionic compound like LHTD4 may have multipotent effects on breast cancer metastasis, the very first of which would be its ability to attenuate EMT and MET of breast cancer cells via inhibiting TGF-β1 and CXCL12–CXCR4-mediated mechanisms, respectively. Further studies are necessary to show the involvement of LHTD4 in attenuating other important signaling pathways that are amenable to cancer metastasis, such as CXCL12/CXCR7 pathway as well as the extent to which the anti-angiogenesis effect of this compound may also contribute in the process of metastasis inhibition. Further studies are necessary to show the involvement of LHTD4 in attenuating other important signaling pathways that are amenable to cancer metastasis, such as CXCL12/CXCR7 pathway, as well as the extent to which the anti-angiogenesis effect of this compound may also contribute in the process of metastasis inhibition. Lastly, a long-term treatment strategy protocol and effective circumvention of the development of chemo-resistance with such strategy also need to be studied.

Disclosure of potential conflict of interest

The authors declare no conflict of interest.

Acknowledgments

This study was supported by grants from the Bio & Medical Technology Development Program (grant no. 2012028833) and the Basic Science Research Program (grant no. 2010-0027955) of the National Research Foundation of Korea (NRF), funded by Korean Ministry of SIP [MSIP].

Appendix A. Supplementary data

Supplementary data related to this article can be found at http://dx.doi.org/10.1016/j.biomaterials.2016.01.058.

References

[1] A. Jemal, F. Bray, M.M. Center, J. Ferlay, E. Ward, D. Forman, Global cancer statistics, CA Cancer J. Clin. 61 (2) (2011) 69–90.
[2] B. Weigelt, J.L. Peterse, L.J. van't Veer, Breast cancer metastasis: markers and models, Nat. Rev. Cancer 5 (8) (2005) 591–602.
[3] E.F. Solomayer, I.J. Diel, G.C. Meyberg, C. Gollan, G. Bastert, Metastatic breast cancer: clinical course, prognosis and therapy related to the first site of metastasis, Breast Cancer Res. Treat. 59 (3) (2000) 271–278.
[4] P. Mehlen, A. Puisieux, Metastasis: a question of life or death, Nat. Rev. Cancer 6 (6) (2006) 449–458.
[5] Y. Kang, P.M. Siegel, W. Shu, M. Drobnjak, S.M. Kakonen, C. Cordon-Cardo, T.A. Guise, J. Massague, A multigenic program mediating breast cancer metastasis to bone, Cancer Cell 3 (6) (2003) 537–549.
[6] T. Imamura, A. Hikita, Y. Inoue, The roles of TGF-beta signaling in carcinogenesis and breast cancer metastasis, Breast Cancer 19 (2) (2012) 118–124.
[7] D. Padua, J. Massague, Roles of TGFbeta in metastasis, Cell Res. 19 (1) (2009) 89–102.
[8] B.L. Eckhardt, P.A. Francis, B.S. Parker, R.L. Anderson, Strategies for the discovery and development of therapies for metastatic breast cancer, Nat. Rev. Drug Discov. 11 (6) (2012) 479–497.
[9] M. Zhang, S. Kleber, M. Rohrich, C. Timke, N. Han, J. Tuettenberg, A. Martin-Villalba, J. Debus, P. Peschke, U. Wirkner, M. Lahn, P.E. Huber, Blockade of TGF-beta signaling by the TGFbetaR-I kinase inhibitor LY2109761 enhances radiation response and prolongs survival in glioblastoma, Cancer Res. 71 (23) (2011) 7155–7167.
[10] Y. Kang, C.R. Chen, J. Massague, A self-enabling TGFbeta response coupled to stress signaling: Smad engages stress response factor ATF3 for Id1 repression in epithelial cells, Mol. Cell 11 (4) (2003) 915–926.
[11] B.I. Dalal, P.A. Keown, A.H. Greenberg, Immunocytochemical localization of

secreted transforming growth factor-beta 1 to the advancing edges of primary tumors and to lymph node metastases of human mammary carcinoma, Am. J. Pathol. 143 (2) (1993) 381–389.
[12] N.S. Nagaraj, P.K. Datta, Targeting the transforming growth factor-beta signaling pathway in human cancer, Expert Opin. Investig. Drugs 19 (1) (2010) 77–91.
[13] D. Padua, X.H. Zhang, Q. Wang, C. Nadal, W.L. Gerald, R.R. Gomis, J. Massague, TGFbeta primes breast tumors for lung metastasis seeding through angiopoietin-like 4, Cell 133 (1) (2008) 66–77.
[14] D. Yao, C. Dai, S. Peng, Mechanism of the mesenchymal-epithelial transition and its relationship with metastatic tumor formation, Mol. Cancer Res. 9 (12) (2011) 1608–1620.
[15] Y.L. Chao, C.R. Shepard, A. Wells, Breast carcinoma cells re-express E-cadherin during mesenchymal to epithelial reverting transition, Mol. Cancer 9 (179) (2010).
[16] M. Kucia, K. Jankowski, R. Reca, M. Wysoczynski, L. Bandura, D.J. Allendorf, J. Zhang, J. Ratajczak, M.Z. Ratajczak, CXCR4-SDF-1 signalling, locomotion, chemotaxis and adhesion, J. Mol. Histol. 35 (3) (2004) 233–245.
[17] B.A. Teicher, S.P. Fricker, CXCL12 (SDF-1)/CXCR4 pathway in cancer, Clin. Cancer Res. 16 (11) (2010) 2927–2931.
[18] J.L. Benovic, A. Marchese, A new key in breast cancer metastasis, Cancer Cell 6 (5) (2004) 429–430.
[19] R.J. Epstein, The CXCL12-CXCR4 chemotactic pathway as a target of adjuvant breast cancer therapies, Nat. Rev. Cancer 4 (11) (2004) 901–909.
[20] M. Simka, T. Urbanek, Anti-metastatic activities of heparins, J. Cancer Mol. 5 (1) (2009) 3–8.
[21] I. Capila, R.J. Linhardt, Heparin-protein interactions, Angew. Chem. Int. Ed. 41 (3) (2002) 391–412.
[22] E.M. Munoz, R.J. Linhardt, Heparin-binding domains in vascular biology, Arterioscler. Thromb. Vasc. Biol. 24 (9) (2004) 1549–1557.
[23] E. Lee, Y.S. Kim, S.M. Bae, S.K. Kim, S. Jin, S.W. Chung, M. Lee, H.T. Moon, O.C. Jeon, R.W. Park, I.S. Kim, Y. Byun, S.Y. Kim, Polyproline-type helical-structured low-molecular weight heparin (LMWH)-taurocholate conjugate as a new angiogenesis inhibitor, Int. J. Cancer 124 (12) (2009) 2755–2765.
[24] D.Y. Lee, S.K. Kim, Y.S. Kim, D.H. Son, J.H. Nam, I.S. Kim, R.W. Park, S.Y. Kim, Y. Byun, Suppression of angiogenesis and tumor growth by orally active deoxycholic acid-heparin conjugate, J. Control Release 118 (3) (2007) 310–317.
[25] K. Park, Y.S. Kim, G.Y. Lee, R.W. Park, I.S. Kim, S.Y. Kim, Y. Byun, Tumor endothelial cell targeted cyclic RGD-modified heparin derivative: inhibition of angiogenesis and tumor growth, Pharm. Res. 25 (12) (2008) 2786–2798.
[26] F. Alam, S.W. Chung, S.R. Hwang, J.Y. Kim, J. Park, H.T. Moon, et al., Preliminary safety evaluation of a taurocholate-conjugated low-molecular-weight heparin derivative (LHT7): a potent angiogenesis inhibitor, J. Appl. Toxicol. 35 (2015) 104–115.
[27] F. Alam, S.R. Hwang, T.A. Al-Hilal, S.W. Chung, H.S. Kim, B.H. Kang, et al., Safety studies on intravenous infusion of a potent angiogenesis inhibitor: taurocholate-conjugated low molecular weight heparin derivative LHT7 in preclinical models, Drug Dev. Ind. Pharm. (2015) 1–11.
[28] S.W. Chung, M. Lee, S.M. Bae, J. Park, O.C. Jeon, H.S. Lee, H. Choe, H.S. Kim, B.S. Lee, R.W. Park, S.Y. Kim, Y. Byun, Potentiation of anti-angiogenic activity of heparin by blocking the ATIII-interacting pentasaccharide unit and increasing net anionic charge, Biomaterials 33 (35) (2012) 9070–9079.
[29] T.A. Al-Hilal, J. Park, F. Alam, S.W. Chung, J.W. Park, K. Kim, et al., Oligomeric bile acid-mediated oral delivery of low molecular weight heparin, J. Control Release 175 (2014) 17–24.
[30] F. Alam, T.A. Al-Hilal, S.W. Chung, D. Seo, F. Mahmud, H.S. Kim, et al., Oral delivery of a potent anti-angiogenic heparin conjugate by chemical conjugation and physical complexation using deoxycholic acid, Biomaterials 35 (2014) 6543–6552.
[31] T.A. Al-Hilal, F. Alam, Y. Byun, Oral drug delivery systems using chemical conjugates or physical complexes, Adv. Drug Deliv. Rev. 65 (2013) 845–864.
[32] T.A. Al-Hilal, S.W. Chung, F. Alam, J. Park, K.E. Lee, H. Jeon, et al., Functional transformations of bile acid transporters induced by high-affinity macromolecules, Sci. Rep. 4 (2014) 4163.
[33] S. Lee, S.K. Kim, D.Y. Lee, K. Park, T.S. Kumar, S.Y. Chae, Y. Byun, Cationic analog of deoxycholate as an oral delivery carrier for ceftriaxone, J. Pharm. Sci. 94 (11) (2005) 2541–2548.
[34] Y.D. Shang, J.L. Zhang, Q.C. Zheng, Natural velvet antler polypeptide conformation prediction and molecular docking study with TGF-beta1 complex, J. Mol. Model. 19 (9) (2013) 3671–3682.
[35] I. Kufareva, B.S. Stephens, L.G. Holden, L. Qin, C. Zhao, T. Kawamura, R. Abagyan, T.M. Handel, Stoichiometry and geometry of the CXC chemokine receptor 4 complex with CXC ligand 12: molecular modeling and experimental validation, Proc. Natl. Acad. Sci. U. S. A. 111 (50) (2014) E5363–E5372.
[36] O. Trott, A.J. Olson, Software news and update AutoDock Vina: improving the speed and accuracy of docking with a new scoring function, efficient optimization, and multithreading, J. Comput. Chem. 31 (2) (2010) 455–461.
[37] J.J. Ziarek, C.T. Veldkamp, F. Zhang, N.J. Murray, G.A. Kartz, X. Liang, J. Su, J.E. Baker, R.J. Linhardt, B.F. Volkman, Heparin oligosaccharides inhibit chemokine (CXC motif) ligand 12 (CXCL12) cardioprotection by binding orthogonal to the dimerization interface, promoting oligomerization, and competing with the chemokine (CXC motif) receptor 4 (CXCR4) N terminus, J. Biol. Chem. 288 (1) (2013) 737–746.
[38] A. Muller, B. Homey, H. Soto, N. Ge, D. Catron, M.E. Buchanan, T. McClanahan, E. Murphy, W. Yuan, S.N. Wagner, J.L. Barrera, A. Mohar, E. Verastegui, A. Zlotnik, Involvement of chemokine receptors in breast cancer metastasis, Nature 410 (6824) (2001) 50–56.
[39] C. Wendel, A. Hemping-Bovenkerk, J. Krasnyanska, S.T. Mees, M. Kochetkova, S. Stoeppeler, J. Haier, CXCR4/CXCL12 participate in extravasation of metastasizing breast cancer cells within the liver in a rat model, PLoS One 7 (1) (2012) e30046.
[40] S. Ali, L.A. Hardy, J.A. Kirby, Transplant immunobiology: a crucial role for heparan sulfate glycosaminoglycans? Transplantation 75 (11) (2003) 1773–1782.
[41] L.X. Ma, H.Q. Qiao, C.J. He, Q. Yang, C.H.A. Cheung, J.R. Kanwar, X.Y. Sun, Modulating the interaction of CXCR4 and CXCL12 by low-molecular-weight heparin inhibits hepatic metastasis of colon cancer, Investig. New Drugs 30 (2) (2012) 508–517.
[42] E.K. Gozansky, J.M. Louis, M. Caffrey, G.M. Clore, Mapping the binding of the N-terminal extracellular tail of the CXCR4 receptor to stromal cell-derived factor-1alpha, J. Mol. Biol. 345 (4) (2005) 651–658.
[43] J.W. Murphy, Y. Cho, A. Sachpatzidis, C. Fan, M.E. Hodsdon, E. Lolis, Structural and functional basis of CXCL12 (stromal cell-derived factor-1 alpha) binding to heparin, J. Biol. Chem. 282 (13) (2007) 10018–10027.
[44] I. Vlodavsky, G. Abboud-Jarrous, M. Elkin, A. Naggi, B. Casu, R. Sasisekharan, N. Ilan, The impact of heparanase and heparin on cancer metastasis and angiogenesis, Pathophysiol. Haemost. Thromb. 35 (1–2) (2006) 116–127.
[45] C.J. Bosques, S. Raguram, R. Sasisekharan, The sweet side of biomarker discovery, Nat. Biotechnol. 24 (9) (2006) 1100–1101.